Scripta Materialia 133 (2017) 79–82

Contents lists available at ScienceDirect

Scripta Materialia

journal homepage: www.elsevier.com/locate/scriptamat

Regular Article

Reverse austenite transformation behavior in a tempered martensite low-alloy steel studied using *in situ* neutron diffraction

Y. Tomota [a,*], W. Gong [b], S. Harjo [c], T. Shinozaki [d]

[a] Research Center for Structure Materials, National Institute for Materials Science, 1-2-1 Sengen, Tsukuba, Ibaraki 305-0047, Japan
[b] Elements Strategy Initiative for Structural Materials, Kyoto University, Yoshida-honmachi, Sakyo-ku, Kyoto 606-8501, Japan
[c] J-PARC Center, Japan Atomic Energy Agency, 2-4 Shirane Shirakata, Tokai-mura, Naka-gun, Ibaraki 319-1195, Japan
[d] Steel Casting and Forging Division, Kobe Steel, Ltd., 2-3-1 Shinhama, Arai, Takasago, Hyogo 676-8670, Japan

ARTICLE INFO

Article history:
Received 17 January 2017
Received in revised form 30 January 2017
Accepted 10 February 2017
Available online xxxx

Keywords:
In situ neutron diffraction
Tempered martensite
Primary extinction
Austenite memory
Nucleation and growth

ABSTRACT

The microstructure evolution during reverse transformation of a Cr-Ni-Mo steel consisting of tempered lath martensite and Cr carbide was examined using *in situ* neutron diffraction at high temperatures. The microstructural change from a reversed coarse-grained structure to a fine-grained polygonal structure by further annealing was monitored through a decrease in the diffraction intensity caused by primary extinction and the full width at half maximum. This result is different from that for a bainite steel, showing good coincidence with the observations using electron back scatter diffraction.

Phase transformation from ferrite (α) to austenite (γ), *i.e.*, reverse transformation, has been utilized to refine the γ grain size in the steel production process. However, the γ grain size after the γ reversion in bainite or martensite steel sometimes becomes as large as that of the prior γ, which is called "γ memory" [1]. This reversed γ with coarse-grains changes to a fine-grained polygonal γ by further high-temperature annealing [2–4], which is similar to recrystallization. The mechanisms of such puzzling phenomena have been studied by many researchers [1,4–7], because it is a serious problem in industrial steel production. Shinozaki et al. have recently reviewed past studies and investigated the mechanism of the γ reversion behavior using *in situ* electron backscatter diffraction (EBSD) [8,9]. Their results on a tempered martensite steel [8,9] and a bainite steel [9] are summarized in Fig. 1, in which (a)–(d) show the tempered martensite steel containing mostly Cr carbides and a little cementite, while (e)–(h) show the bainite steel containing cementite particles. As observed, austenite grains nucleated during the reverse transformation are categorized into two types, A and B. The microstructures of Fig. 1(b) and (f) consist fully of austenite, in which examples of type B grains are indicated by red arrows. In Fig. 1(b), small number of type B equiaxed grains are scatted in the type A grains with lath shape (the matrix: see ref. 8 for more details). On the other hand, type B grains are dominantly observed in Fig. 1(f). For type A, γ grains nucleated at the lath boundaries with almost the same crystal orientation as that of the prior γ grain, whereas for type B, the γ grains nucleated at the prior γ grain boundaries or inside the prior γ grains with different crystal orientations. Type A grains are characterized by high kernel average misorientation (KAM) values, as seen in Fig. 1(c) and (g); on the other hand, the type B grains show very low KAM values (see red arrows in Fig. 1(c) and (g)). The most likely nucleation site inside the grain is the cementite particle. In the case of the tempered martensite steel, type A nucleation occurs predominantly because of the presence of a little cementite. Therefore, after the γ reverse transformation was completed, the prior γ grains were reconstructed by the growth of type A grains as seen in Fig. 1(b), which is called the γ memory phenomenon. As was discussed in ref. 8, this reverse transformation was not displacive (martensitic) but diffusional. Here, sub-boundaries remaining in such a reconstructed γ grain originally stemmed from the small-angle lath-boundaries of martensite (for details, see ref. 8). Hence, by heating to a higher temperature, type A grains were invaded and eventually replaced by type B grains, resulting in a new fine-grained polygonal microstructure; this is similar to recrystallization behavior. These two types of γ nucleation are also observed in the bainite steel, as shown in Fig. 1(e)-(h). Different from the tempered martensite, type B grains nucleate predominantly in the bainite steel, so that a fine-grained γ structure appeared immediately after the completion of the γ reversion without showing γ memory. These are the main results recently obtained by surface observations with EBSD experiments [8,9], and this tentative conclusion is expected to be confirmed by evidence in the bulk, because the chemical

* Corresponding author.
E-mail address: TOMOTA.Yo@nims.go.jp (Y. Tomota).

http://dx.doi.org/10.1016/j.scriptamat.2017.02.017
1359-6462/

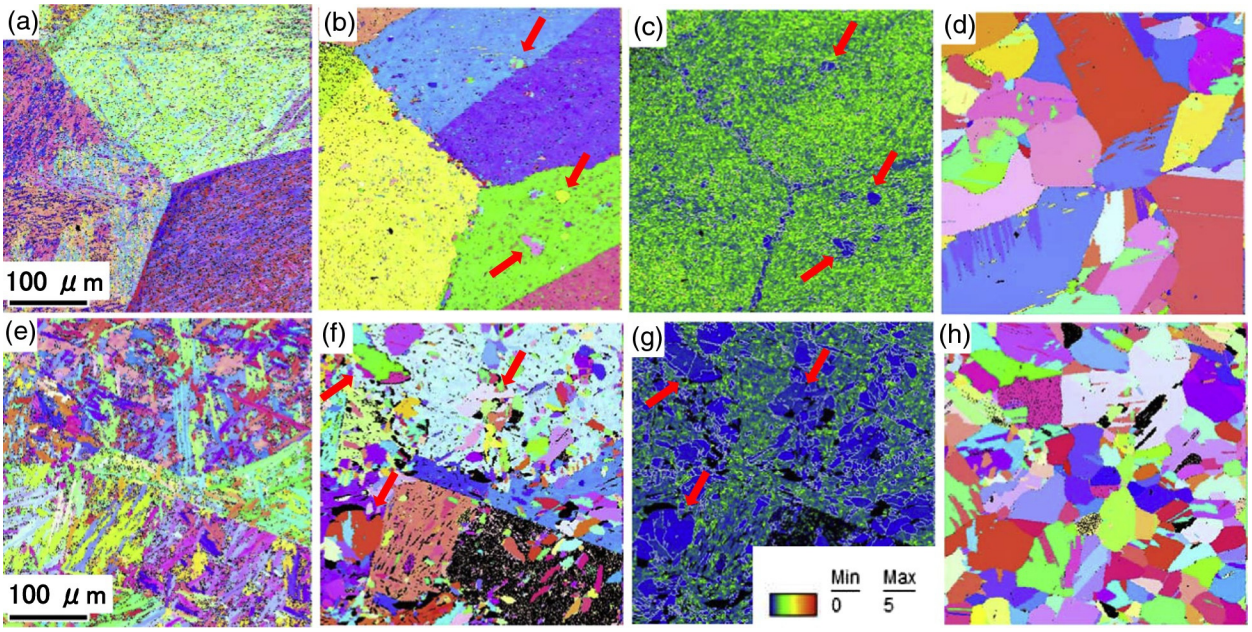

Fig. 1. EBSD results: (a)-(d): tempered martensite steel, (e)-(h) bainite steel; (a) and (e): 923 K (before reverse transformation), (b) 1148 K and (f) 1078 K (after reverse transformation), (c) and (f) KAM maps of (b) and (f), respectively, and (d) 1173 K and (h) 1153 K (after growth of austenite grains).

compositions, particularly Mn and C, at the surface layer were suspected to change at elevated temperatures. Therefore, *in situ* neutron diffraction was employed in this study to monitor the γ reversion behavior of the tempered martensite steel using a bulk specimen.

The same steel as that used in Fig. 1(a)-(d) was used in this study. The chemical composition of the steel was 0.36C-0.22Si-0.79Mn-0.007P-0.003S-3.04Cr-1.46Ni-0.43Mo-0.1 V-0.03Al (mass%) and balance Fe. The specimen was annealed at 1453 K for 3.6 ks, followed by quenching in water, and then the quenched specimen was tempered at 973 K for 54 ks with the aim of the precipitating the alloy carbides and the decomposing the retained γ. The Ac_1 and Ac_3 temperatures determined by dilatometry were 1003 K and 1088 K, respectively.

In situ neutron diffraction measurements were performed during the heat treatment using a time-of-flight (TOF) neutron diffractometer, TAKUMI at the Materials and Life Science Facility (MLF) in the Japan Proton Accelerator Research Complex (J-PARC). A cylindrical specimen with 8 mm in diameter and 30 mm in length was prepared. The neutron diffraction patterns in the axial and transverse directions were measured simultaneously using two detector banks having scattering angles of $\pm 90°$. The gauge volume was restricted to $5 \times 5 \times 5$ mm^3 using an incident beam slit and radial collimators. The TAKUMI instrumental peak width, *i.e.*, wavelength resolution, was ~0.3% for the medium resolution mode used in this experiment. A thermocouple was welded on the specimen surface to measure and control the temperature. Heat treatment was conducted in vacuum to avoid oxidation. The specimen was heated at a heating rate of 1 K/s from 293 K (RT) to 993 K (before the start of reverse transformation) and held there for 1.2 ks, then heated up to 1048 K at 0.05 K/s and held there for 1.2 ks, then to 1193 K (after the completion of γ reverse transformation), 1143 K, and finally 1223 K, in that order. The heat schedule is depicted in Fig. 2(a). The two-dimensional (2D) plots of the diffraction intensities of 111 γ, 200 γ, and 110 α peaks are presented in Fig. 2(b) as a function of the annealing time. As seen, it is found that the temperature range for α-to-γ transformation is almost consistent with that from Ac_1 to Ac_3 determined by dilatometry [8]. Here, both the diffraction peak intensity and full width at half maximum (FWHM) apparently decrease from 1143 K to 1223 K after becoming a single γ phase, which will be discussed later in detail. This corresponds to the EBSD results observed in Fig. 1(b)-(d). Diffraction profiles (the axial direction) collected for 0.6 ks at the latter half of the isothermal holding at 1143 K and 1223 K are presented in Fig. 2(c). It is observed that the diffraction intensities of all the hkl peaks at 1223 K are smaller than those observed at 1143 K (see red arrows in the figure). Here the 200 peaks at the two temperatures were magnified in order to show the differences clearly; the peak shift due to thermal expansion, a large decrease in the maximum intensity and a small change of line profile broadening are found.

The detailed changes in the diffraction intensities and FWHMs of some hkl peaks obtained in the axial direction are shown in Fig. 3(a) and (b), respectively. The plotted values were obtained by time slicing of every 60 s for the event-mode recorded date and all the hkl peak intensities and FWHMs were normalized to the intensities and FWHMs at the beginning of holding the temperature at 1093 K, respectively. The peak intensities were found to drastically decrease upon heating from 1160 K to 1200 K (Fig. 3(a)). The lowest indexed peak of 111 (at the largest wavelength) shows the most significant drop in peak intensity (larger than 50%), while the drop in a higher indexed peak like 311 is small, in which the large scatters are due to its low absolute diffraction intensity. Similar drops in the hkl diffraction intensities were also observed in the results for the transverse direction. Therefore, such simultaneous drops in all peak intensities cannot be explained by a change in the texture. In the case of texture evolution, the diffraction intensities of some peaks would become stronger, whereas the others would become weaker. Kabra et al. observed a similar decrease in the neutron diffraction intensities of all the hkl peaks for the α-to-β transformation in a zirconium alloy and explained it by the effect of the primary extinction of the incident beam [10]. They have claimed that the increase in crystal perfection driven by thermal recovery causes a transition from the kinematic to the dynamic theory of diffraction. The wavelength dependence observed in Fig. 3(a) can also be explained by the effect of primary extinction. Another possible origin of the decrease in all the peaks intensities is the effect of the Debye-Waller factor, but Kabra et al. have disregarded it because the amount of decreasing is estimated to be very small (approximately 5%) and its wavelength dependence is different from the primary extinction (the opposite trend) [10]. Hence, the results in Fig. 3(a) must be due to the primary extinction of the incident beam at elevated temperatures related to the growth of type B grains,